

UNCLASSIFIED

Defense Technical Information Center  
Compilation Part Notice

ADP012466

TITLE: Comparison of the 120-MM M831A1 Projectile's Experimental Launch Dynamic Data with Hydrocode Gun-Projectile Dynamic Simulations

DISTRIBUTION: Approved for public release, distribution unlimited

This paper is part of the following report:

TITLE: 10th U.S. Army Gun Dynamics Symposium Proceedings

To order the complete compilation report, use: ADA404787

The component part is provided here to allow users access to individually authored sections of proceedings, annals, symposia, etc. However, the component should be considered within the context of the overall compilation report and not as a stand-alone technical report.

The following component part numbers comprise the compilation report:

ADP012452 thru ADP012488

UNCLASSIFIED

# COMPARISON OF THE 120-MM M831A1 PROJECTILE'S EXPERIMENTAL LAUNCH DYNAMIC DATA WITH HYDROCODE GUN- PROJECTILE DYNAMIC SIMULATIONS

K. P. Soencksen,<sup>1</sup> J. F. Newill,<sup>1</sup> J. M. Garner,<sup>1</sup> and P. Plostins<sup>1</sup>

<sup>1</sup>U.S. Army Research Laboratory, AMSRL-WM-BC, Aberdeen Proving Ground, MD 21005

This paper documents experimental validation for numerical simulations using the U.S. Army Research Laboratory's (ARL) gun-projectile dynamic simulation codes. The experimental program was conducted at ARL's Transonic Range Experimental Facility on the M831A1 high-explosive antitank (HEAT) training projectile for the M256 gun system. The experimental program consisted of the M831A1 HEAT training projectile fired for the measurement of aerodynamic characteristics. Measured first maximum yaw levels are compared to simulated data for the same system. The effect of damage tubes to help explain occasional launch anomalies is also shown.

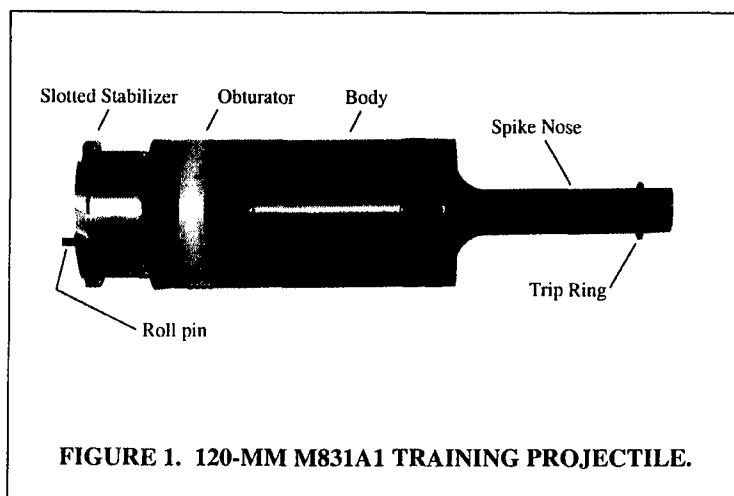
## 1. INTRODUCTION

The 120-mm M831A1 projectile is a low-cost training projectile used by U.S. armor troops. The M831A1 training ammunition program is managed by the Operations Support Command (OSC) at Rock Island, IL, which is supported by the U.S. Army Armament Research, Development, and Engineering Center (ARDEC) at Picatinny Arsenal, NJ. The M831A1 is used as a surrogate training round for high-explosive antitank (HEAT) M830 and M830A1 service rounds. In 1994, the M831A1 replaced the M831 projectile. The M831A1 resulted in significant cost savings to the government since the boom and fins of the M831 were replaced with a simple slotted stabilizer. Today the round is produced by two government contractors, each producing approximately 50% of the rounds purchased by the Army. A photograph of the M831A1 is shown in Figure 1.

The M831A1, a full-bore projectile, provides a unique analytical opportunity for an analysis of the type examined here since it is not a sabot projectile. This means that the projectile enters free flight very near the muzzle, and the muzzle rates are not modified by sabot discard. Since the muzzle rates are the same as the rates entering free flight, direct comparison between the muzzle rates predicted by the gun codes and those measured in experiments is straight forward.

The M831A1 is fired from the M1A1 tank in large numbers annually by training armor crews. As with all projectile types, a computer correction factor (CCF) or fleet zero is used in the tank's fire control system to account for average fleet projectile jump. For the last several years, the OSC (formerly the Industrial Operations Command, IOC) has received feedback from the user that, in some cases, M831A1 impact performance did not appear consistent with the current M831A1 CCF. Based on this information, the OSC and ARDEC sought a low-scale but in-depth experimental analysis of the round to assess its aeroballistic qualities and to hopefully identify any potential issues that could affect accuracy. The five-shot experiment was conducted at the Transonic Experimental Facility (TEF) operated by the Aerodynamics Branch of the U.S. Army Research Laboratory (ARL), Aberdeen Proving Ground, MD.

Concurrently, funding was provided to initiate in-depth computer simulation analyses of the interior ballistic characteristics of the M831A1.



Specifically, the effects of bore erosion and bore centerline were examined as to their potential effect on projectile dynamic path and angular rates at muzzle exit. This paper first presents the experimental methodology and data leading to the indirect measurement of projectile first maximum yaw. The first maximum yaw is central in this study since it is a proportional indicator of angular rates at the muzzle for a nonsaboted projectile like the M831A1. Next, a direct comparison is made between the performance predictions obtained from the simulation study and the experimental data obtained from the range.

## 2. TEST SETUP AND METHODOLOGY

The test was fired from an M1A1 main battle tank equipped with a 120-mm M256 gun system, tube serial number 3700. This tube did display some damage, which is key to the findings of this paper, and will be discussed later. All five rounds were fired through the TEF's spark range facility containing 25 orthogonal shadowgraph stations. An interior view of the range is shown in Figure 2. From the figure, camera positions are noted along the left-hand wall of the range facility and in pits along the range floor. The camera stations are arranged in five groups of five stations each along a trajectory length of approximately 183 m. Opposite each camera is a large reflective screen, as seen on the right-hand wall and ceiling in the figure. As the flight projectile approaches a station, an infrared sensor detects the projectile just uprange of the station and sends a signal to the station camera with a preset delay time based on the expected projectile velocity. After the delay time has elapsed, a high-intensity spark source is initiated. Each camera is carefully focused on the screen, and thus the shadow of the projectile is captured in flight.

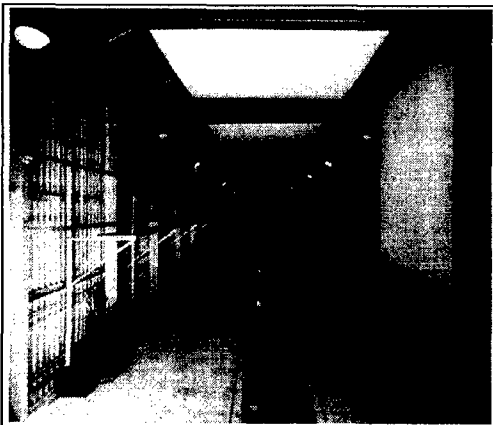


**FIGURE 2. INTERIOR VIEW, TRANSONIC EXPERIMENTAL FACILITY.**

Figure 3 shows a shadowgraph of the M831A1, which is representative of those recorded from the test. The image shows the M831A1 at a moderate angle-of-attack, 4.4 deg. From this, we see the basic flowfield encountered by the projectile, including the shock pattern and boundary layer. Note the thin vertical line just to the right of the projectile nose. This is the image of the fiducial cable which is tightly suspended in a surveyed position about 25-mm from the surface of each station screen. Attached to the cable are fiducial beads, two of which are evident in the figure just above the nose tip. The surveyed locations of the cable and beads are used to determine the exact position and orientation of the projectile in each plane, at each shadowgraph station. Careful examination of Figure 3 in the vicinity of the projectile base reveals the shadow of a roll pin. This is a small pin inserted in the base of the projectile (see Figure 1) that is used to measure roll orientation. Measurements of the position of the roll pin in each shadowgraph are used to derive the roll history, allowing for the calculation of roll-related aerodynamics, as described further below.

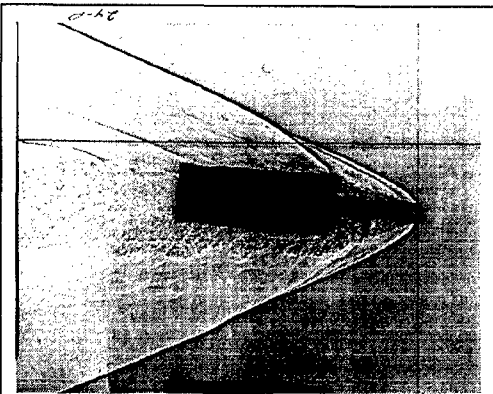


**FIGURE 3. SHADOWGRAPH, SHOT 2, 102 M,  $M=3.1$ , ANGLE=4.4 DEG.**

As stated, first maximum yaw is central to the study presented here since it is a proportional indicator of angular rates present at the muzzle. However, first maximum yaw is not directly measured experimentally. This is because the range shadowgraph stations begin approximately 38 m downrange of the gun muzzle. Thus, once the six-degree-of-freedom (6-DOF) fit to the data is computed, the fit is extrapolated uprange to the muzzle providing the approximate first maximum yaw magnitude and orientation. Accuracy of these values depends on accuracy of the fit, which, in turn, depends on accuracy of the position and orientation measurements.

Since the range facility generally yields highly accurate position and orientation measurements, the first maximum yaw is typically accurate to within 0.1 deg.

### 3. EXPERIMENTAL DATA REDUCTION AND RESULTS

This section describes the important aerodynamic coefficients of a projectile and presents details of how they were calculated. Accurate calculation of the pertinent coefficients is a prerequisite to determining the actual flight dynamics (position and orientation) anywhere along the trajectory.

Aeroballistic flight qualities are described by the set of aerodynamic coefficients. These are calculated using the Aeroballistic Research Facility Data Analysis System (ARFDAS) code written and supported by Arrowtech Associates (Whyte and Hathaway 1981). This code uses an inverse routine that fits the measured projectile angle and position data first to the linearized equations of motion and then to the full 6-DOF equations of motion and computes the aerodynamic forces and moments required to have produced the measured flight. Integral to this routine is the input of roll orientation, which allows calculation of the static roll moment coefficient,  $C_{l_0}$ , and roll damping moment coefficient,  $C_{l_p}$ . These coefficients are then used in the 6-DOF motion analysis to improve the accuracy in determining other aerodynamic coefficients.

The ARFDAS code also supports a multiple-fit capability that allows the computation of a single set of aerodynamic parameters using the data from multiple shots. This allows the estimation of aerodynamic coefficients with higher confidence levels.

In addition to the obvious advantage of obtaining more accurate coefficients, the multiple-fit capability has another powerful benefit. Frequently, a projectile flight occurs with low level motion in terms of both angle of attack (AOA) and center of gravity (CG) motion (swerve). While such a trajectory is highly desirable in a tactical engagement, low-levels of motion result in the measurement errors being similar in magnitude to the actual motion. Hence, less accurate aerodynamic coefficients are computed. Thus, in the experimental environment, ballisticians desire at least moderate AOA and CG motions. When such motions are not present for a particular shot, aerodynamic coefficients usually cannot be accurately derived from the data set. However, as in the case of the current study, there is usually a need to reasonably determine the projectile yaw and swerve history. This can be obtained, in turn, by utilizing the accurate aerodynamic coefficients that have been computed from multiple fits of the data of other shots containing larger motions. Usually, this procedure improves the relative knowledge about the yaw and CG motion history of a low-yaw shot, providing at least an order of magnitude assessment of some important trajectory characteristics such as first maximum yaw.

Moreover, occasionally in range experiments, instrumentation malfunction or flight anomalies yield only sparse shadowgraph data for a particular shot. As in the case previously described, the coefficients obtained from multiple fits of the data of other shots containing more complete data often allow a user to determine approximate trajectory characteristics much more accurately than with the sparse data of a particular shot.

### 4. AERODYNAMIC COEFFICIENTS

A comprehensive analysis was performed on the data from all five shots using the ARFDAS code as previously described. First, a best fit was obtained to the measured position and angle data using the linearized equations of motion. From this, a "first cut" group of aerodynamic coefficients was obtained. Next, this data was used as initial input for the 6-DOF computations. Here, the aerodynamic coefficients were adjusted to provide the best data fit to the full 6-DOF equations of motion. The aerodynamic coefficient data resulting from the analysis for zero-yaw drag, pitching moment, normal force, and pitch damping moment are presented next.

First, zero-yaw drag is plotted in Figure 4. Since drag is easily and accurately measured, all five individual data points fall on a line with minimal scatter. All shots were fired without tracers; thus, the drag coefficients determined would likely be a few percent higher than those obtained from any other testing in which traced rounds were fired. The solid circle data points represent multiple fits in which the reduction routine is constrained to compute a single value of drag coefficient for the data of multiple shots. In the case of zero-yaw drag,  $C_{x_0}$ , the coefficient value is not enhanced by the multiple-fit capability, since the coefficients obtained from the individual shots are so accurate to begin with. The data are in excellent agreement with predicted values computed by the PRODAS design code. Two wind tunnel data points are also shown for

comparison (Farina 1998). Although not plotted, the first and second nonlinear drag components are obtained with greater-than-anticipated accuracy. This was possible because of several shots that exhibited moderate-to-high yaw levels. The average value determined for  $C_{X_{\alpha 2}}$  is 29.8, with a probable error of just 2.1%; and that for  $C_{X_{\alpha 4}}$  is -530, with a probable error of 6.2%. These values, previously unknown, are somewhat different from predicted values.

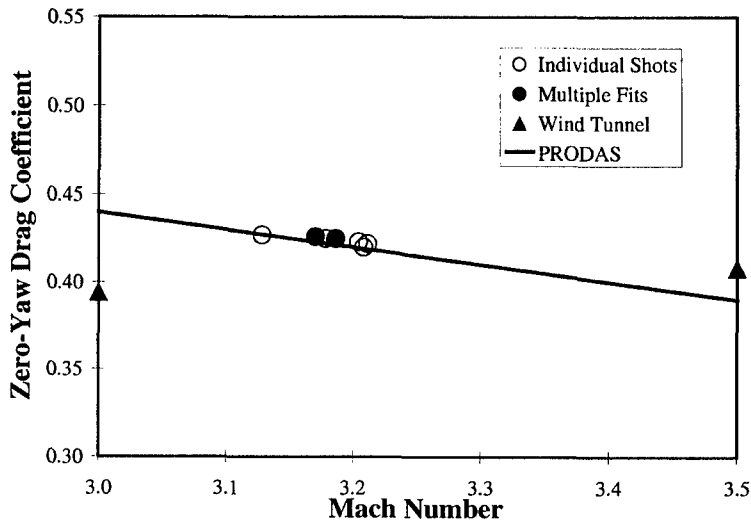


FIGURE 4. ZERO-YAW DRAG VS. MACH NUMBER.

Pitching moment coefficient,  $C_{m_{\alpha}}$ , is plotted in Figure 5.

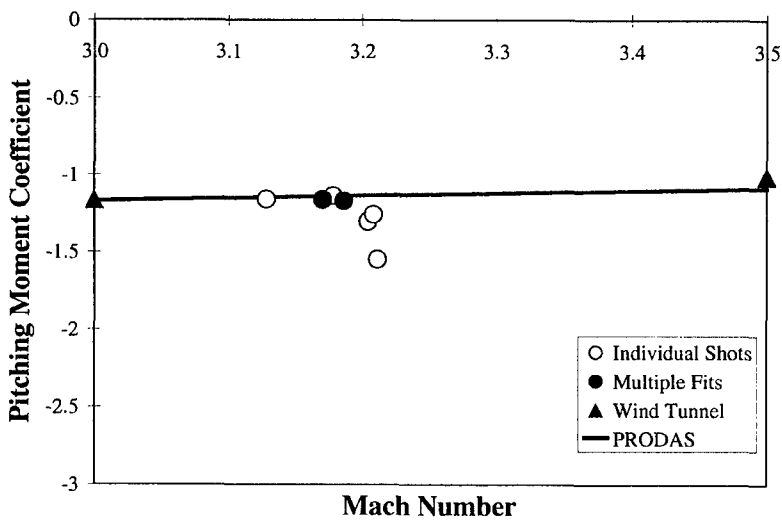


FIGURE 5. PITCHING MOMENT COEFFICIENT VS. MACH NUMBER.

As in the case of drag, the individual data points show little scatter, and both the PRODAS predicted values and wind tunnel data match very well with the experimental data. The value of  $C_{m_{\alpha}}$  for Shot 3 is -1.54, the most different from the multiple-fit values. This can be attributed to the low yaw on this shot, resulting in a less accurate determination of  $C_{m_{\alpha}}$ . Note that the pitching moment coefficient values are much smaller

than what is typical for a statically stable projectile due to its relatively lower static margin. The cubic pitching moment coefficient,  $C_{m\alpha^3}$ , is determined to be  $-5.2$ , with a 10% probable error.

The normal force coefficient,  $C_{N\alpha}$ , is plotted in Figure 6. Only multiple-fit values of the coefficient are plotted, since individual shot data produced fairly significant scatter. This is because accurately calculating the coefficient is a function of the amount of projectile swerve (cg motion). Three shots in particular result in poor  $C_{N\alpha}$  values; these all have swerve arm magnitudes that are significantly smaller than those of the other two shots, thus leading to more error in these values. The analysis of  $C_{N\alpha}$  offers validation of the value of the multiple-fit reductions. Again, both wind tunnel data and PRODAS predictions match well with the experimental free-flight numbers.

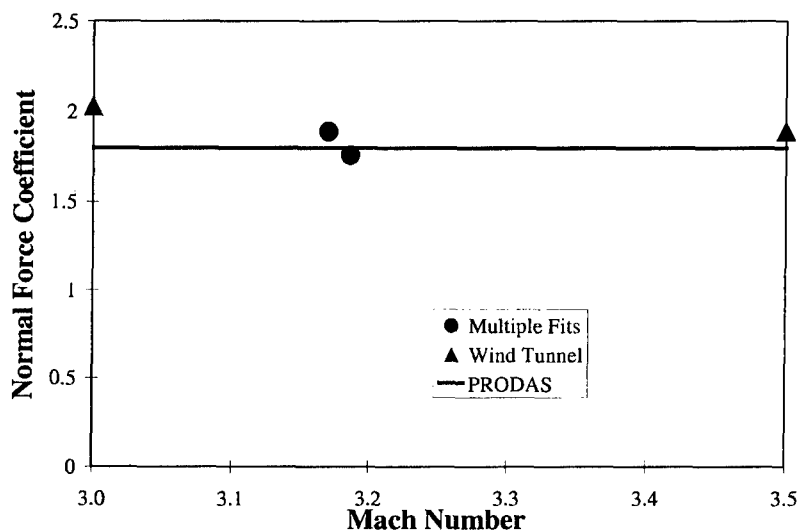


FIGURE 6. NORMAL FORCE COEFFICIENT VS. MACH NUMBER.

Finally, Figure 7 plots multiple-fit values of the pitch damping moment coefficient,  $C_{mq}$ . Accurately computing  $C_{mq}$  depends on the yaw magnitude, the amount of change in the yaw magnitude, the number of complete yaw cycles measured. In general, the greater the yaw magnitude and the more cycles that are measured, the more accurate the pitch damping coefficient will be. However, even for high yaw shots in which several complete yaw cycles are measured, if the overall *change* in yaw level with range is small, then damping characteristics are very difficult to accurately extract. This was the case with Shot 2 of the current experiment, which exhibits very high yaw levels. Despite high yaw and approximately 3.5 yaw periods of measured flight, the yaw level stays nearly constant with range. In other words, damping is neutral; hence, an accurate pitch damping moment coefficient is indeterminate. The same type of phenomenon is observed in three other shots that display marginal pitch damping characteristics. In all three cases, a low yaw level, a minimal *change* in yaw with range (marginal damping), or a combination of both result in  $C_{mq}$  values with high probable errors. One shot produces a calculated  $C_{mq}$  of  $-12.4$  with low yaw, but the amount of damping present allows a somewhat reasonable probable error of 25%. This data point is not plotted, but this value is consistent with the PRODAS prediction. Even the multiple-fit values of  $C_{mq}$  result in very high probable errors, again because the relative amount of damping is very small. This fact provides further confirmation that an accurate value for pitch damping moment coefficient is not possible from the current data set. However, the experimental data analysis clearly indicates that marginal pitch damping exists; therefore, the PRODAS-predicted value might be optimistic.

Table 1 presents a summary of aerodynamic coefficient values (determined from multiple-fit data analysis) with their associated probable errors. In addition to the coefficients listed in the table, a complex analysis is conducted in an attempt to determine the roll-related coefficients: static roll moment coefficient,  $C_{r0}$ , and roll damping moment coefficient,  $C_{rp}$ . Details of this analysis, beyond the scope of this work, are presented by Soenksen et al. (2001).

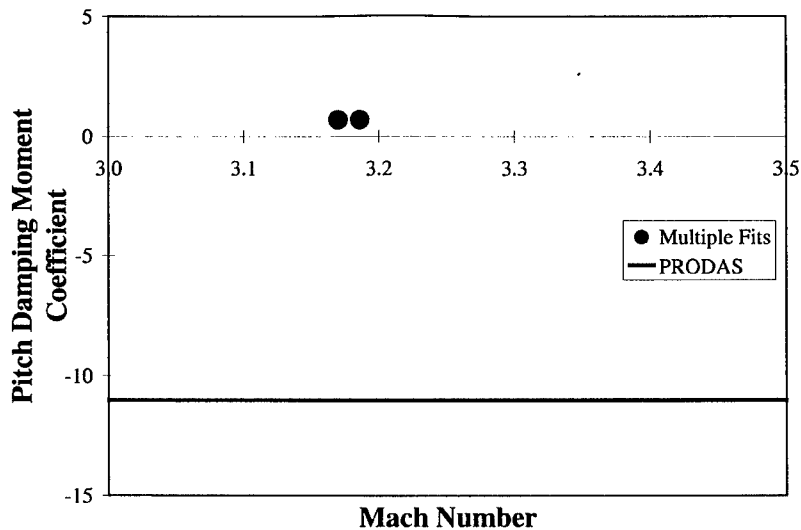


FIGURE 7. PITCH DAMPING MOMENT COEFFICIENT VS. MACH NUMBER.

TABLE 1. AERODYNAMIC COEFFICIENTS.

Coefficient	Value	Probable Error (%)
<b>Drag</b>		
Zero-Yaw ( $C_{X0}$ )	0.425	0.1
Squared Component ( $C_{Xa2}$ )	29.8	2.1
Quad Component ( $C_{Xa4}$ )	-530	6.2
<b>Pitching Moment</b>		
Linear ( $C_{ma}$ )	-1.17	0.9
Cubic Component ( $C_{ma3}$ )	-5.2	9.9
<b>Normal Force</b>	1.8	3.8
<b>Pitch Damping Moment</b>	1	**

\*\* Probable error too high for reliable value.

Several interesting observations are gleaned from plots of the projectile yawing motion, as produced by the 6-DOF fits to the position and orientation data. The yawing motion in orthogonal planes is plotted in Figure 8 for Shot 1.

In this and subsequent yaw plots, the gun muzzle is located 38 m uprange of the first spark station (marked by a vertical line near the left-hand edge of the plot), and the sign convention is positive up and left. This plot shows the experimental data points in each plane, together with the computed best fits from the 6-DOF solution to the equations of motion. Notice that the pitch angle peaks grow slightly with range, while the yaw angle peaks appear to be approximately constant. When this angular data is combined into total AOA, the plot shown in Figure 9 results.

Here, all yaw maxima and minima are evident to about 220 m. Note that the first maximum yaw (about 1.65 deg) is greater than the second maximum yaw, as expected. The third maximum yaw, however, is greater than both the first and second maxima. In general, a slightly growing step-like pattern is displayed.

A similar step-like pattern is seen when examining the yaw minima. This is indicative of an aerodynamic trim angle, as described by Soencksen et al. (2000). The magnitude of the stepping motion is possibly slightly less than that indicated by the total yaw fit. This is hypothesized because of the fit error inherent in any data-fitting procedure and is based on the fact that some data points are underpredicted by the fit curve. Despite the uncertainty in its exact magnitude, the stepping phenomenon of the yawing motion is definitely present and significant enough to be measurable. More importantly, identification of the presence of aerodynamic trim is critical to the accurate extrapolation of the fit to determine first maximum yaw. Had the trim not been isolated, the first maximum yaw would probably have been slightly underpredicted in this case.

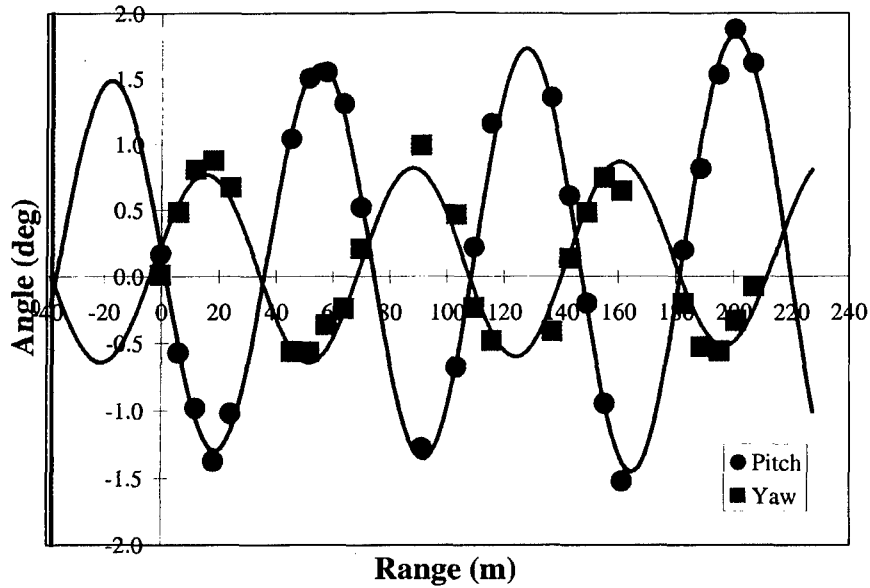


FIGURE 8. PITCH AND YAW VS. RANGE, SHOT 1.

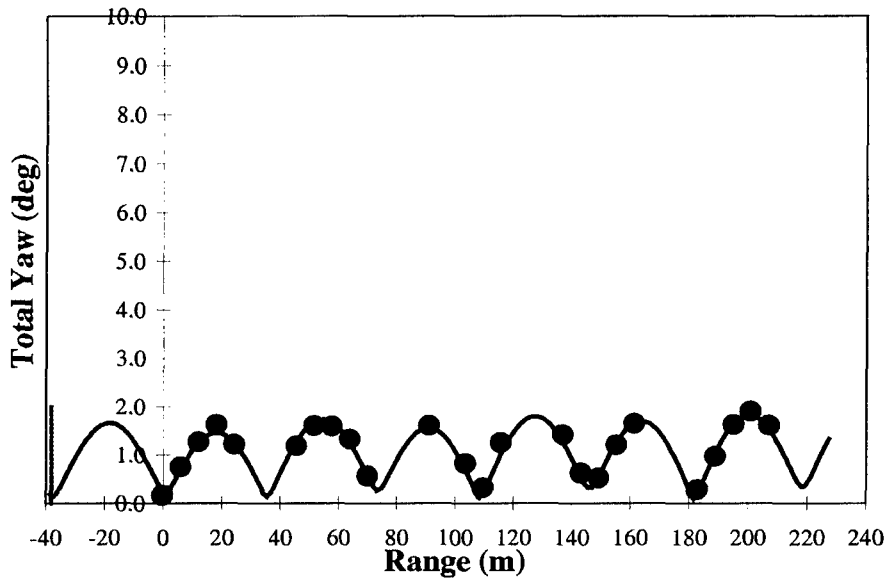


FIGURE 9. TOTAL YAW VS. RANGE, SHOT 1.

The total AOA did not display any visible stepping motion on Shot 2, as shown in Figure 10, but evidence of aerodynamic trim is again found in Shots 3 – 5. The total AOA is plotted for these shots in Figure 10 and Figure 11. The yawing motion for Shot 3 is so small that a good quality fit to the data is not obtained, even using multiple-fit aerodynamic coefficients. The first maximum yaw for this shot is almost certainly less than 0.5 deg.

A fair amount of variability in the yaw levels from shot to shot is noted. The first maximum yaw varies from less than 1 deg to over 9 deg for these shots.

Analysis of yaw data shows evidence of the presence of a trim vector of varying magnitude for four out of the five shots. Computed trim angle values for all shots are presented in Table 2. Agreement is good between the independent calculations of linear theory and 6-DOF. Inclusion of the computed trims in the angular fits results in improved fit errors, and thus more accurate first maximum yaw values, in all cases except Shot 2, where trim is not a significant factor.

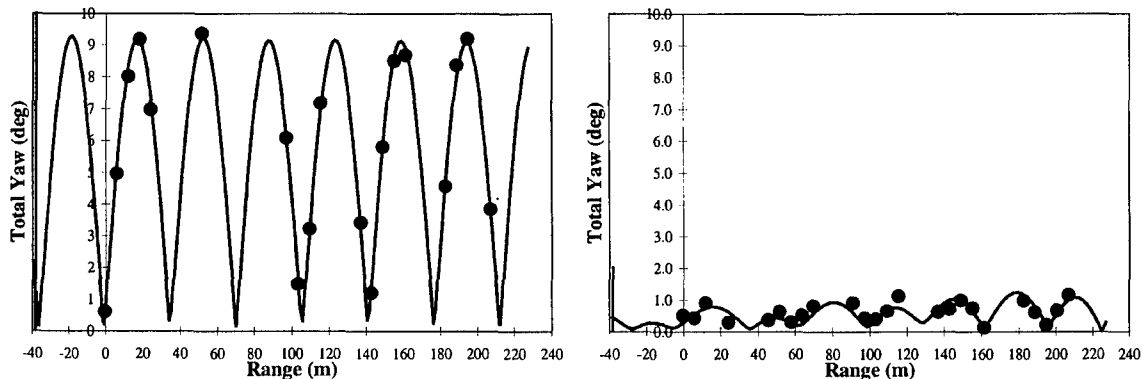


FIGURE 10. TOTAL YAW VS. RANGE, SHOT 2 AND 3.

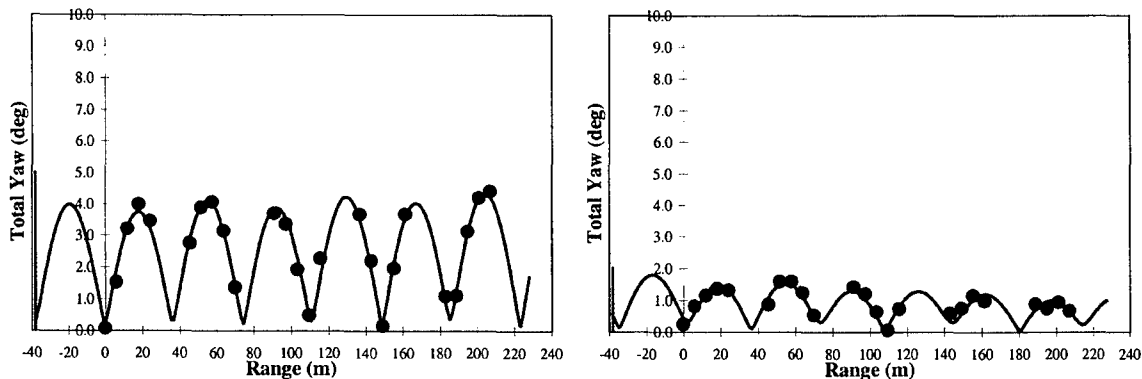


FIGURE 11. TOTAL YAW VS. RANGE, SHOT 4 AND SHOT 5.

TABLE 2. CALCULATED TRIM ANGLES.

Shot	Linear Theory Trim (deg)	6-DOF Trim (deg)
1	0.114	0.136
2	0.001	0.038
3	0.257	0.264
4	0.108	0.171
5	0.162	0.149

### 5. NUMERICAL SIMULATION OF TANK GUN PROJECTILES

Gun/projectile dynamic simulations utilize three-dimensional (3-D) finite element (FE) models of the M256 120-mm tank cannon launching projectiles. The method is described in Rabern 1991; Wilkerson and Hopkins 1994; Burns et al. (1998); Newill et al. (1998a); Newill et al. (1998b, 1998c, 1998d, 1999a, 1999b, 2000); Guidos et al. (1999). The hydrocode finite element formulation was chosen to allow investigation of

stress wave propagation due to elements of launch. The models are 3-D to capture the asymmetric response of the projectile and gun system resulting from the nonlinear path of the projectile during launch, asymmetric boundary conditions, general lack of symmetry in the centerline profiles of the gun tube, and asymmetric gun motion. Figure 12 shows the solid models used to simulate the M831A1.

The projectiles and gun systems are both built in similar manners. Models are developed for the components and then integrated. Relative motion is obtained by defining the proper physics to allow interaction between the parts. Since this projectile is relatively simple, the nose, body, stabilizer, and obturator are welded together, and sliding interfaces are defined between the nose, body, stabilizer, and the gun bore. The propellant pressure loading for the gun system and projectile is generated from IBHVG2 (Anderson and Fickie 1987), which provides good quality interior ballistic prediction for production charges.

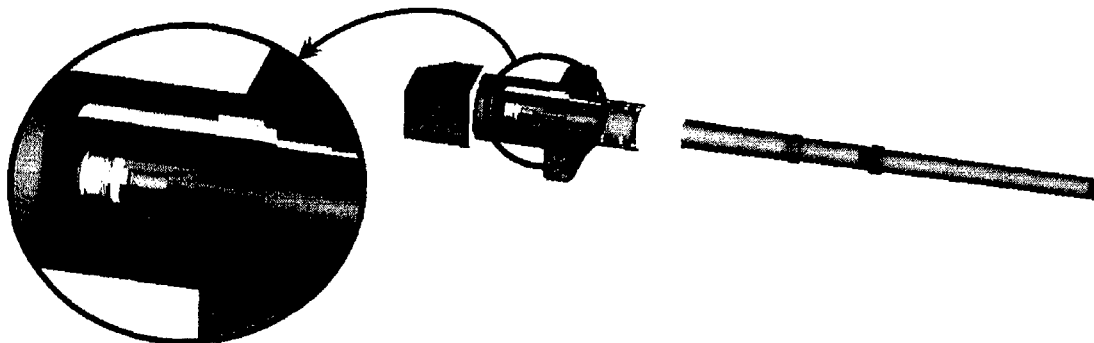
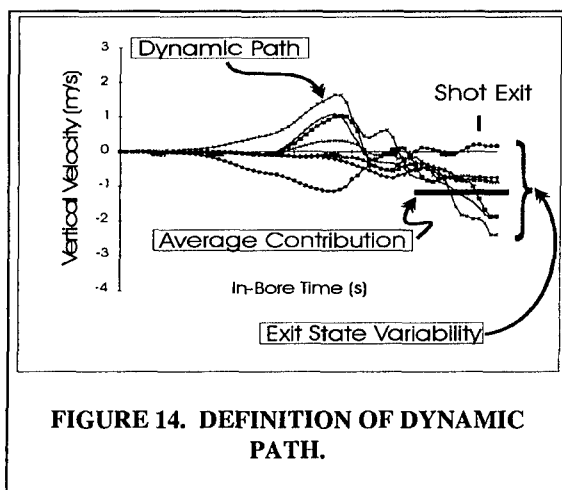
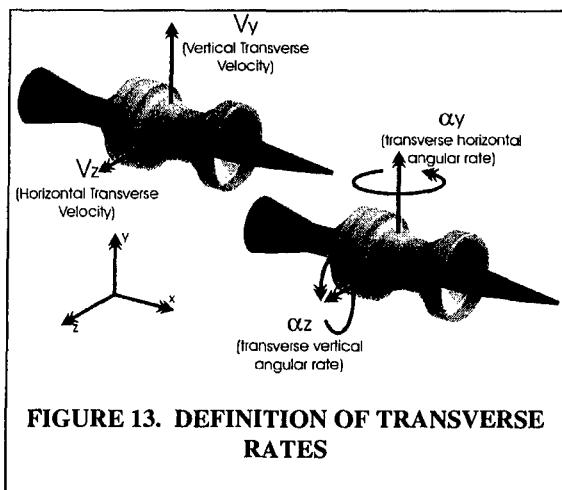


FIGURE 12 M1'S M256 GUN SYSTEM WITH KE PROJECTILE SHOWN IN-BORE.

The gun dynamic simulation codes predict the transverse rates (linear and angular, see Figure 13) during the launch cycle. Three types of information are used from these predictions: the dynamic path, variability in jump, and the average jump. These are illustrated in Figure 14. The dynamic path gives qualitative information on the rate history of the projectile during the launch cycle. The variability and average jump predicted by the codes are related to accuracy errors where reduction in variability or error represents improved performance of the system. It should be noted that the simulations used the same gun tube profiles as the experiments at TEF.



In order to validate the gun codes, some type of methodology is required in order to compare simulation results to experiments. Since the phenomena being predicted are nonlinear and stochastic in nature and the initial conditions are not known precisely on a shot-by-shot basis, the gun dynamic codes are used to predict an envelope of performance, which is comparable to the groups fired during the experiment.

It is very important to note that a firing experiment is a ballistic phenomenon that is not entirely predictable. Even with production ammunition, and with as many factors as possible controlled, there can be significant deviation of the shooting performance. For this reason, a direct comparison between the simulated data and the experimental data is very difficult.

Figure 15 and Figure 16 show the dynamic paths from the simulations. The dynamic paths show that the projectile motion is relatively low transverse motion for approximately the first one third of the in-bore cycle. When the projectile begins reacting to the gun system, it exhibits moderate balloting behavior. The projectile exits the gun bore at approximately 8.8 ms (ambient conditioned propellant).

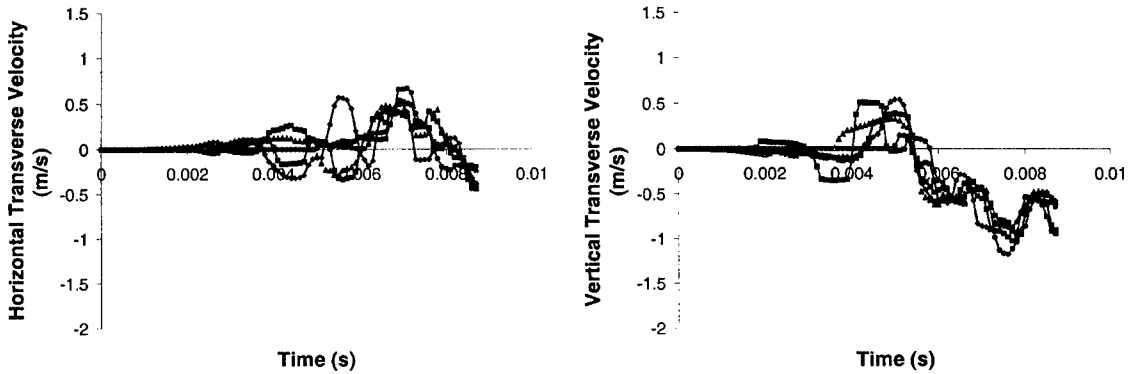


FIGURE 15. TRANSVERSE VELOCITY VS TIME.

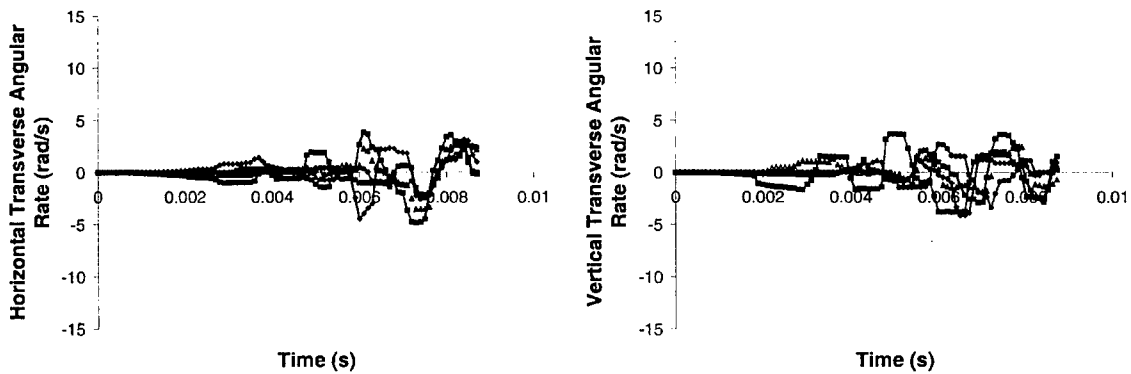


FIGURE 16. ANGULAR RATE VS TIME.

The simulation data is compared to the experimental data by predicting the first maximum yaw from the angular rate data at the muzzle seen in the dynamic path plots. The rates are converted using equation (1) with the constants provided as determined from the experiment.

$$\alpha_{1^{st} \max} = \frac{|\alpha_{\text{muzzle}}|}{\omega}, \quad \omega = \frac{V_{\text{muzzle}}}{d \sqrt{\frac{c_{m\alpha} \pi \rho d^5}{8I_{\text{transverse}}}}} \quad (1)$$

$$d = 0.11968 \text{ m}, \rho = 1.225 \text{ kg/m}^3, c_{m\alpha} = -1.2,$$

$$I_{\text{transverse}} = 0.1427 \text{ kg m}^2, V_{\text{muzzle}} = 1165 \text{ m/s}$$

The values of the first maximum yaw predicted by the gun codes are up to 1.7 deg. The comparison between the simulation data and the experimental data is given in Figure 17. The figure shows the first maximum yaw measured during the TEF test, along with two ranges of simulation data, represented by two shaded regions. The first region is a grey rectangular box near the bottom of the figure. This is the range of first maximum yaw values predicted by the codes for a pristine gun tube. The upper patterned region shows the degradation of these results when the simulations incorporate some effects of bore erosion damage (Newill et al. 2001).

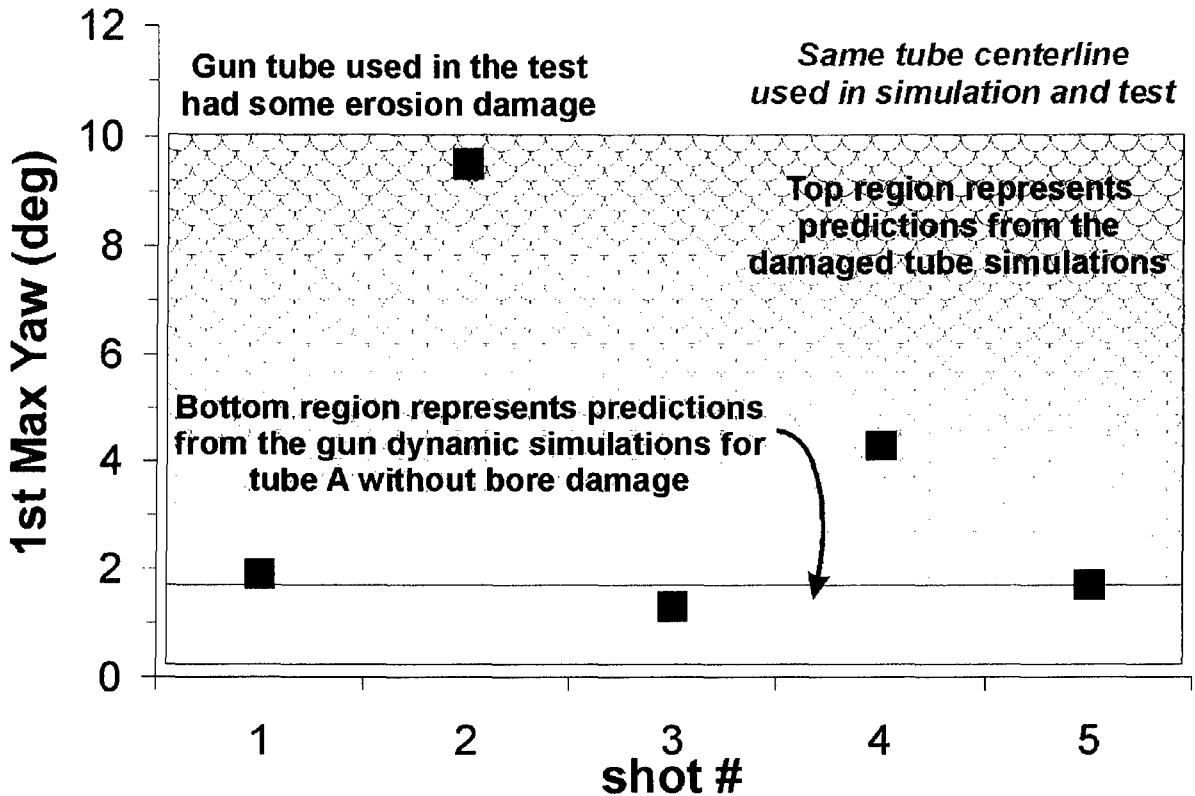


FIGURE 17. SIMULATION COMPARISON WITH EXPERIMENTAL RESULTS.

The predictions were modified to include damage because the experiment was fired using a gun tube with some bore damage. This test was conducted concurrently with another experimental program, and consequently, the other program drove the choice of the gun tube. No attempt was made to map the bore or simulate the exact damage in the gun tube as this is beyond the capability of the codes utilized.

The data showed reasonable agreement between the experiment and the simulations. The use of a gun tube with erosion in the experiment introduced some ambiguity when compared to the simulations. One of the shots, # 2, experienced a large launch disturbance out of the normal distribution of launch rates of the projectile. This shot showed that something abnormal occurred during the in-bore portion of the launch, implying that all the shots in the experiment may have been disturbed to some extent.

## 6. CONCLUSIONS

The data and analysis presented in this report are the result of the first free-flight, highly instrumented and analyzed experiment conducted on the M831A1 training projectile, combined with a detailed assessment

of numerous computer simulations. This work was a significant step toward a more comprehensive understanding of the complex aerodynamic phenomena affecting the performance characteristics of the M831A1.

Experimental yawing motion was determined accurately in most cases. First maximum yaw displayed significant variability from shot to shot, with the first maximum yaw of one shot reaching over 9 deg. Another shot displayed moderate yaw levels, while the remaining three exhibited relatively low levels. For a nonsaboted projectile, launch dynamics alone were the source of the yaw that grew immediately from the muzzle, eventually peaking at the first maximum yaw. These were a direct combined result of all in-bore phenomena affecting the projectile and giving it both angular and cg rates at the muzzle.

Detailed computer simulation analyses yielded predictions of first maximum yaw based on computed muzzle angular rates. Agreement with the experimental data was good, although comparison had to be made both with and without damage. The results of the simulation provided a high degree of confidence that the models were performing correctly.

Erratic launch dynamics as observed experimentally (and predicted in simulation) provided a potential explanation for the occasional anomalous rounds observed by the user in training.

## 7. ACKNOWLEDGEMENTS

The magnitude of this study required a coordinated effort and support from many people. The principal organizations involved were ARL, ARDEC, OSC, Alliant Techsystems Inc, General Dynamics Ordnance and Tactical Systems. Their leadership, expertise and experience were invaluable. This study relied heavily on supercomputers supplied by the Department of Defense's High Performance Computing initiative (specifically by the Major Shared Resource Center at the ARL).

## 8. REFERENCES

- Anderson, R. D., and K. D. Fickie. "IBHVG2 - A User's Guide." BRL-TR-2829, U.S. Army Ballistic Research Laboratory, Aberdeen Proving Ground, MD, Jul 1987.
- Bornstein, J., I. Celmins, and P. Plostins, "Launch Dynamics of Fin-Stabilized Projectiles." AIAA Paper No. 89-3395, Aug 1989.
- Bornstein, J., I. Celmins, P. Plostins, E. M. Schmidt. "Techniques for the Measurement of Tank Cannon Jump." BRL-MR-3715, U.S. Army Ballistic Research Laboratory, Aberdeen Proving Ground, MD, Dec 1988.
- Bundy M. L., J. F. Newill, and C. P. R. Hoppel, "A Notional Redesign of the M865E3 Obturator." M. L. Bundy, J. F. Newill, and C. P. R. Hoppel, ARL-TR-2325, Sep 00.
- Bundy M., J. Newill, V. Marcopoli, M. Ng, C. Wells, "A Methodology for Characterizing Barrel Flexure Due to Tank Motion." ARL-MR-479, Jun 00
- Burns B. P., D. L. Henry, C. D. McCall, and J. F. Newill, "Flexural Characteristic of the M829 Projectile Family." ARL-TR-1201, APG, MD, Sep 96.
- Burns B. P., J. F. Newill, and S. A. Wilkerson, "In-Bore Projectile Gun Dynamics." Proceedings of the 17th International Ballistics Symposium, Midran, South Africa, 26 Mar 98.
- Demitroff, D. Personal communication first two authors. Alliant Techsystems, Hopkins, MN December 1999-2000.
- Dohrn, R. Personal communication first two authors. Alliant Techsystems, Hopkins, MN December 1999-2000.
- Durkin, P. Personal communication first two authors. Aberdeen Test Center, Aberdeen Proving Ground, MD December 1999.
- Guidos B., P. Plostins, D. Webb, J. F. Newill, "120-mm Tank Gun Accuracy Demonstrator (TGAD) Jump Test," ARL-TR-29, Dec 99.
- Hathaway, W. Personal communication. Arrowtech Associates, South Burlington, VT December 1999.
- Hoppel C.P.R., J. F. Newill, and K. P. Soenksen, "Evaluation of Obturator and Sealing Cuff Properties for the M865 Training Projectile with Comparison to Ballistic Testing," ARL-TR-2039, APG, MD, Sep 99.
- Lyon, D. H. "Radial Stiffness Measurements of 120-mm Tank Projectiles." ARL-TR-392, U.S. Army Research Laboratory, Aberdeen Proving Ground, MD, Apr 94.
- Lyon, D. H. and K. P. Soenksen. "Radial Stiffness and In-Bore Balloting Analysis for the M900 Projectile." ARL-TR-593, U.S. Army Research Laboratory, Aberdeen Proving Ground, MD, Oct 94.
- Manole, L. Personal communication. U.S. Army Research Development and Engineering Center, Picatinny Arsenal, NJ December 1999.
- Murphy, C.H. "Free Flight Motion of Symmetric Missiles." BRL-MR-1216, U.S. Army Ballistic Research Laboratory Technical Report, Aberdeen Proving Ground, MD July 1963.
- Newill J. F., B. P. Burns, and S. A. Wilkerson, "Overview of Gun Dynamics Numerical Simulations," ARL-TR-1760, APG, MD, Sep 98a.
- Newill J. F., C. P. R. Hoppel, D. Kamdar, B. Guidos, and B. Drysdale, C. Livecchia, and M. Luciano, "Geometric and Material Changes to the Forward Bourrelet to Optimize Performance of KE Ammunition," ARL-TR-2328, Sept 00.

- Newill J. F., C. P. R. Hoppel, K. P. Soencksen, and P. Plostins, "Simulation of the M865 Kinetic Energy Projectile with Experimental Validation." Proceedings of the 18th International Ballistics Symposium, San Antonio, TX, Nov 99a.
- Newill J. F., C. P. R. Hoppel, W. H. Drysdale, and D. S. Kamdar, "Effects of Bourrelet Stiffness on the Interior Ballistic Performance of Kinetic Energy Ammunition." ARL-TR-02, APG, MD, Jun 99b.
- Newill J. F., C. P. R. Hoppel, W. H. Drysdale, and S. A. Wilkerson "Numerical Simulation of Launch Interaction of Kinetic Energy Long Rod Fin-Stabilized Projectiles and M1A1 Abrams M256 Gun System with Comparison to Experimental Results." National Def. Industrial Assoc. 48th Annual Bomb & Warhead Technical Symp., Eglin Air Force Base, FL. May 11-14, 98b.
- Newill J. F., C. P. R. Hoppel, and W. H. Drysdale, "Comparison of Launch Mechanics and Dynamics from the M1A1 M256 Gun System for the M829A2 Kinetic Energy Long Rod Fin Stabilized Projectile Containing Different Penetrator Materials." ARL-TR-1671, APG, MD, Apr 98c.
- Newill J. F., S. A. Wilkerson, C. P. R. Hoppel, and W. H. Drysdale. "Numerical Simulation of Composite Kinetic Energy Projectiles Launched by an M1A1 Abrams M256 Gun System." Proceedings of the 30th SAMPE Technical Conference, San Antonio, TX, 23 Oct 98b.
- Newill, J. F., D. Webb, B. Guidos, C. P. R. Hoppel, and W. H. Drysdale. "Methodology for Formal Comparison of Experimental Ballistic Firing of Kinetic Energy Projectiles With Numerical Simulation." Technical Report, U.S. Army Research Laboratory, Aberdeen Proving Ground, MD, in progress.
- Plostins, P., I. Celmins, and J. Bornstein. "The Effect of Sabot Front Borerider Stiffness on the Launch Dynamics of Fin-Stabilized Kinetic Energy Ammunition." AIAA Paper No. 90-0066, Jan 90.
- Rabern D.A., "Axially Accelerated Saboted Rods Subjected to Lateral Forces," Ballistic Research Laboratory Contractor Report No. 671, Aug 91.
- Schmidt, E. M., P. Plostins, and M. Bundy. "Flash Radiographic Diagnostics of Projectile Launch from Cannon." Proceedings of Flash Radiography Symposium, E.A. Webster, Jr. and A.M. Kennedy, editors., The American Society for Nondestructive Testing, 1984.
- Soencksen K., J. F. Newill, P. Plostins, "Aerodynamics of the 120-mm M831A1 Projectile: Analysis of Free-Flight Experimental Data," Proceedings of AIAA Atmospheric Flight Mechanics Conference & Exhibit, Denver, AIAA-00-4198, CO, 14-17 Aug, 00
- Soencksen, K. P., J. F. Newill, J. M. Garner, and P. Plostins, "Comparison of the 120-mm M831A1 Projectile's Experimental Launch Dynamic Data with Hydrocode Gun-Projectile Dynamic Simulations." 10th U. S. Army Gun Dynamics Symposium, Austin, TX, 23 - 26 Apr 01
- Soencksen, K.P., J.F. Newill, P. Plostins, "Aerodynamics of the 120-mm M831A1 Projectile: Analysis of Free-Flight Experimental Data," Proceedings of the AIAA Atmospheric Flight Mechanics Conference & Exhibit, 14-17 August, 2000, Denver, CO.
- Soencksen, K.P., J.F. Newill, P. Plostins, "Roll Characteristics of the 120-mm M831A1 Projectile," Proceedings of the 39th AIAA Aerospace Sciences Meeting & Exhibit, 8-11 January 2001, Reno, NV.
- Whirley R. G., D. E. Englemann, and J. O. Hallquist. "DYNA3D; A Nonlinear, Explicit, Three-Dimensional Finite Element Code for Solid and Structural Mechanics - User's Manual" Lawrence Livermore's National Laboratory, UCRL-MA-107254 Rev 1, Nov 93.
- Whyte, R., Hathaway, W., "Free Flight Range Data Reduction - ARFDAS User's Manual," General Electric Co., Armament & Electrical Systems Department, Burlington, VT, March 1981.
- Whyte, R., W. Hathaway, and J. Groth. "Aeroballistic Characteristics of the M831A1 Determined from Doppler Radar Data." Arrowtech Associates Technical Report, South Burlington, VT August 1994.
- Wilkerson S. A. and D. Hopkins, "Analysis of a Balanced Breech System for the M1A1 Main Gun System Using Finite Element Techniques," Army Research Laboratory Technical Report 608, Nov 94.